

# SU(3) Quantum Interferometry with single-photon input pulses

Si-Hui Tan,<sup>1,\*</sup> Yvonne Y. Gao,<sup>2</sup> Hubert de Guise,<sup>3</sup> and Barry C. Sanders<sup>4</sup>

<sup>1</sup>*Data Storage Institute, 5 Engineering Drive 1, Singapore 117608*

<sup>2</sup>*Department of Physics and Applied Physics, Yale University, New Haven, Connecticut 06520, USA*

<sup>3</sup>*Department of Physics, Lakehead University, Thunder Bay, ON P7B 5E1, Canada*

<sup>4</sup>*Institute for Quantum Information Science, University of Calgary, Alberta, Canada T2N 1N4*

(Dated: August 29, 2012)

We develop a framework for solving the action of a three-channel passive optical interferometer on single-photon pulse inputs to each channel using SU(3) group-theoretic methods, which can be readily generalized to higher-order photon-coincidence experiments. We show that features of the coincidence plots vs relative time delays of photons yield information about permanents, immanants, and determinants of the interferometer SU(3) matrix.

PACS numbers:

An optical interferometer is a coherent scatterer of light comprising passive optical elements such as phase shifters, mirrors, and beam splitters. The interferometer operates in the quantum regime by injecting nonclassical light into the input ports and yields nonclassical light from the output ports. The most famous quantum optical effect is the two-photon Hong-Ou-Mandel (HOM) dip [1], with the “dip” corresponding to extinction of photon-coincidences at the two output ports of a balanced beam splitter given two identical input photons at each input ports. Instead the two photons exit in a superposition state of leaving together from each of the two output ports. Important applications include characterizing distinguishability between pairs of independent photons [2], measuring coherence [3] and purity [4] of single photons, producing two-photon entanglement [5], performing dense coding [6] and single-qubit quantum fingerprinting [7], and creating non-deterministic nonlinear gates in optical quantum computing [8].

Generalizing to higher-order photon-coincidence dips will be valuable in many ways including determining distinguishability between multiple photons simultaneously, computing the permanent of special unitary (SU) matrices through photon coincidence dips [9], and efficiently sampling permanents of sub-matrices of SU matrices, which would be hard classically (with complexity BPP<sup>#P</sup>)[10]. Experimentally eight individual photons have been manipulated with exquisite control [11], and three photons in three coupled interferometers have shown nonclassical interference [12] so higher-order photon coincidence dips are feasible well beyond the two-photon two-channel case. Although coherent scattering of Fock states has been analyzed theoretically for various instances of interferometers [13–15], a full multimode analysis of multi-channel interferometry incorporating realistic source and detector spectral responses and allowing for arbitrary configurations has not yet been fully studied despite its necessity for quantitative studies of these nonclassical interferometric systems.

Here we use group theory to solve the general prob-

lem of photon coincidence probabilities at the output of any passive three-channel interferometer (whose action is represented by the SU(3) matrix) acting on single-photon pulse inputs, and we show specifically how the three-photon coincidence dip can be generated. We exploit the fact that an input of at most one photon per mode yields an output state that is a superposition of states of irreducible representations (irreps) of SU(3), and we find that, conditioned on one photon per mode in the input and output with frequencies unpermuted, the amplitude of the transformation equals a sum of the permanent, immanants and determinant of the SU(3) matrix. Then extinguishing this weighted sum is a necessary and sufficient condition for a three-photon dip.

To illustrate we construct one instance of a SU(3) interferometer coincidence-rate dip by extinguishing the coincidence corresponding to one photon exiting each of the three output ports by judiciously choosing the eight generalized Euler angles. Our results suggest a rich group-theoretic structure to photon interferometry and a direct relationship to permutation symmetries of matrices. Furthermore our methods create a pathway to solving for arbitrary  $n$ -mode interferometers rather than restricting to three modes as reported here.

A single photon pulse with light-source spectral function  $\tilde{\phi}^S(\omega)$  in one spatial mode, or channel, is

$$|1\rangle^S = \int d\omega \tilde{\phi}^S(\omega) |1(\omega)\rangle, \quad \int d\omega |\tilde{\phi}^S(\omega)|^2 = 1 \quad (1)$$

for  $|1(\omega)\rangle \equiv \hat{a}^\dagger(\omega) |0\rangle$  with  $\hat{a}(\omega)$  the creation operator at frequency  $\omega$  satisfying  $[\hat{a}_k(\omega_i), \hat{a}_l^\dagger(\omega_j)] = \delta_{kl}\delta(\omega_i - \omega_j)\mathbb{1}$ ,  $k$  and  $l$  labels for distinct channels, and  $\mathbb{1}$  the identity operator. The parenthetical (rounded) bra-ket notation distinguishes frequency-explicit states from other states. For convenience, we choose a Gaussian spectral functions

$$\tilde{\phi}(\omega) = (2\pi\sigma_0^2)^{-1/4} \exp[-(\omega - \omega_0)^2/(4\sigma^2)], \quad (2)$$

but our approach accommodates any physical spectral function.

The detector has a response function  $\tilde{\phi}^D(\omega)$ , possibly different for each output port. For convenience we take  $\tilde{\phi}^D(\omega)$  to be Gaussian, similar to (2), but perhaps with different mean and variance; the variance is inversely related to the detector integration time. For

$$|n\rangle := \frac{1}{\sqrt{n!}} \left( \prod_{j=1}^n \int d\omega_j \tilde{\phi}^D(\omega_j) \hat{a}^\dagger(\omega_j) \right) |0\rangle \quad (3)$$

an  $n$ -photon state corresponding to a superposition of single-photon states in different infinitesimal frequency modes, the ideal detector executes projective measurements of the type  $\Pi_n := |n\rangle\langle n|$ ,  $\sum_{n=0}^{\infty} \Pi_n = \mathbb{1}$ . Detector inefficiency arises due to a spectral mismatch between source and detector spectral functions: the probability of detecting a single source photon is  $\left| \int d\omega [\tilde{\phi}^S(\omega)]^* \tilde{\phi}^D(\omega) \right|^2 \leq 1$ .

We assume identical photons from the source, with distinguishability introduced by time delays of the pulses. A tunable time delay of  $\tau$  on the single-photon pulse is expressed in the Fourier domain by a phase shift  $|1\rangle \mapsto \int d\omega \tilde{\phi}(\omega) \exp[-i\omega\tau] |1(\omega)\rangle$ , and the inverse Fourier transform of  $\tilde{\phi}(\omega) \exp[-i\omega\tau]$  is  $\phi(t - \tau)$ .

Now that we have established the single-mode source and detector formalism, we consider two photons impinging on the two input ports of the passive two-channel SU(2) interferometer resulting in a photon-coincidence dip. This transformation can be expressed as

$$R(\Omega) = \begin{pmatrix} e^{-i(\alpha+\gamma)} \cos \frac{\beta}{2} & -e^{-i(\alpha-\gamma)} \sin \frac{\beta}{2} \\ e^{i(\alpha-\gamma)} \sin \frac{\beta}{2} & e^{i(\alpha+\gamma)} \cos \frac{\beta}{2} \end{pmatrix} \quad (4)$$

with  $\Omega$  comprising the three Euler angles  $\alpha, \beta, \gamma$ , and the optical-element transformations are assumed to be independent of frequency.

The input state  $|11\rangle^S$  has one photon in each port, i.e., a tensor product of two single-photon source states (1) with time delay  $\tau$  between modes 1 and 2. As we need to convert the direct product of irreps for single-photon interferometer inputs to a direct-sum decomposition, Young tableaux are valuable, especially for SU( $n$ ) interferometry with  $n > 2$  as these cases can be complicated to construct. Young tableaux are diagrams comprising  $\square$ s arranged in rows and columns that represent various partitions of  $n$ .

The representation of any SU(2) matrix on two photons with frequencies  $\omega_1$  and  $\omega_2$  decomposes as

$$\begin{array}{c} \square \otimes \square \rightarrow \square\square \oplus \begin{array}{|c|} \hline \square \\ \hline \end{array} \\ (1,0) \otimes (1,0) \rightarrow (2,0) \oplus (0,0) \end{array} \quad (5)$$

with the second row giving the standard labels of the irreps in terms of highest weight. The decomposition is also written as  $3 \oplus 1$  with  $\ell = 0, 1$  irreps (singlet and triplet, respectively) and  $m = -\ell, \dots, \ell$ .

The two-photon state is a combination of  $|\ell m\rangle$  states:  $|1(\omega_1)1(\omega_2)\rangle = \frac{1}{\sqrt{2}}(|00\rangle + |10\rangle)$ . The single-photon state  $\hat{a}_1^\dagger(\omega_i)|0\rangle$  transforms under SU(2) as  $|\ell = \frac{1}{2} m = \frac{1}{2}\rangle_i$  and  $\hat{a}_2^\dagger(\omega_i)|0\rangle$  transforms as  $|\ell = \frac{1}{2} m = -\frac{1}{2}\rangle_i$ :

$$\begin{aligned} R(\Omega) \hat{a}_1^\dagger(\omega_1) |0\rangle &= \left[ \hat{a}_1^\dagger(\omega_1) D_{\frac{1}{2}, \frac{1}{2}}^{\frac{1}{2}}(\Omega) + \hat{a}_2^\dagger(\omega_1) D_{-\frac{1}{2}, \frac{1}{2}}^{\frac{1}{2}}(\Omega) \right] |0\rangle \\ R(\Omega) \hat{a}_2^\dagger(\omega_2) |0\rangle &= \left[ \hat{a}_1^\dagger(\omega_2) D_{\frac{1}{2}, -\frac{1}{2}}^{\frac{1}{2}}(\Omega) + \hat{a}_2^\dagger(\omega_2) D_{-\frac{1}{2}, -\frac{1}{2}}^{\frac{1}{2}}(\Omega) \right] |0\rangle \end{aligned} \quad (6)$$

with  $D_{m'm}^\ell(\Omega) := \langle \ell m' | R(\Omega) | \ell m \rangle$  an element of the  $(2\ell + 1)$ -dimensional Wigner  $D$ -matrix. The two-photon transformation is thus

$$R(\Omega) |1(\omega_1)1(\omega_2)\rangle = \frac{1}{\sqrt{2}} (R(\Omega) |00\rangle + R(\Omega) |10\rangle). \quad (7)$$

Extinguishing coincidences arising from the triplet  $|10\rangle$  contribution, which is symmetric under an  $\omega_1 \leftrightarrow \omega_2$  exchange, requires that  $\langle 10 | R(\Omega) | 11 \rangle = \frac{1}{\sqrt{2}} D_{00}^1(\Omega) = \cos \beta = 0$ . Therefore,  $\beta = \frac{1}{2}\pi$  and is independent of  $\alpha, \gamma$ . These parameters correspond to a balanced beam splitter with a relative phase shift between modes 1 and 2. For  $\alpha = \pi/4 = -\gamma$ , the beam splitter is balanced and symmetric:  $B := R(\Omega)$  for this important case.

Typically detectors at different output ports are dissimilar. If the source pulse has carrier frequency  $\omega_0$  and bandwidth  $\sigma_0$ , and detectors have carrier frequencies  $\omega_i$  and bandwidths  $\sigma_i$  for each output mode  $i$ , we introduce weighted variances  $\overline{\sigma_i^2} := \sigma_0^2 + \sigma_i^2$ ,

$$\overline{\varsigma_i^2} := \frac{\sigma_i^2 \omega_0 + \sigma_0^2 \omega_i}{\sigma_0^2 + \sigma_i^2}, \quad \widetilde{\sigma_i^2} := \left( \frac{1}{\sigma_0^2} + \frac{1}{\sigma_i^2} \right)^{-1},$$

and Gaussian spectral mismatch function

$$\Lambda_i \equiv \frac{1}{\overline{\sigma_i^2} \sqrt{\widetilde{\sigma_i^2}}} \exp \left( -\frac{(\omega_0 - \omega_i)^2}{2 \overline{\sigma_i^2}} \right). \quad (8)$$

The two-mode output coincidence rate is

$$P_{11} = {}^S \langle 11 | B^\dagger \Pi_1 \otimes \Pi_1 B | 11 \rangle^S \quad (9)$$

$$= \Lambda_1 \Lambda_2 \left| e^{-\tau^2 / \widetilde{\sigma_1^2}} e^{i\tau \overline{\varsigma_1}} - e^{-\tau^2 / \widetilde{\sigma_2^2}} e^{i\tau \overline{\varsigma_2}} \right|^2, \quad (10)$$

$P_{11} = 0$  as expected for indistinguishable photons and identical detectors.

Now we proceed to three-channel SU(3) interferometry transformation, with the eight-parameter generalized Euler angle  $\Omega$  (assumed to be frequency-independent) and factorization [16]

$$\begin{aligned} R(\Omega) &\equiv R_{23}(\alpha_1, \beta_1, -\alpha_1) R_{12}(\alpha_2, \beta_2, -\alpha_2) \\ &\times R_{23}(\alpha_3, \beta_3, -\alpha_3) e^{-i\gamma_1 \hat{h}_1} e^{-i\gamma_2 \hat{h}_2}, \end{aligned} \quad (11)$$

$$\hat{h}_1 = 2\hat{C}_{11} - \hat{C}_{22} - \hat{C}_{33}, \quad \hat{h}_2 = \frac{1}{2}(\hat{C}_{22} - \hat{C}_{33}), \quad \hat{C}_{ij} := \hat{a}_i^\dagger \hat{a}_j,$$

with  $SU(2)$  subgroup matrices

$$R_{23}(\alpha, \beta, -\alpha) = \begin{pmatrix} 1 & 0 & 0 \\ 0 & \cos \frac{\beta}{2} & -e^{-i\alpha} \sin \frac{\beta}{2} \\ 0 & e^{i\alpha} \sin \frac{\beta}{2} & \cos \frac{\beta}{2} \end{pmatrix}, \quad (12)$$

$$R_{12}(\alpha, \beta, -\alpha) = \begin{pmatrix} \cos \frac{\beta}{2} & -e^{-i\alpha} \sin \frac{\beta}{2} & 0 \\ e^{i\alpha} \sin \frac{\beta}{2} & \cos \frac{\beta}{2} & 0 \\ 0 & 0 & 1 \end{pmatrix}. \quad (13)$$

We employ Young tableaux methods to determine output states given the three-photon input state

$$|111\rangle^S = \int d\omega_1 \int d\omega_2 \int d\omega_3 \tilde{\phi}(\omega_1) \tilde{\phi}(\omega_2) \tilde{\phi}(\omega_3) \times e^{i\omega_2 \tau_1} e^{i\omega_3 \tau_2} |1(\omega_1)1(\omega_2)1(\omega_3)\rangle^S \quad (14)$$

with time delays  $\tau_1$  and  $\tau_2$  between modes 1 and 2 and between modes 1 and 3, respectively. The three-photon input state (14) is

$$\begin{array}{c} \square \otimes \square \otimes \square \rightarrow \begin{array}{c} \square \square \square \\ \square \square \square \end{array} \oplus \begin{array}{c} \square \square \\ \square \square \end{array} \oplus \begin{array}{c} \square \square \\ \square \square \end{array} \oplus \begin{array}{c} \square \\ \square \\ \square \end{array} \\ (1,0) \otimes (1,0) \otimes (1,0) \rightarrow (3,0) \oplus (1,1) \oplus (1,1) \oplus (0,0) \end{array} \quad (15)$$

with the second row giving the standard labels in terms of highest weight. The last element of (15) is the fully antisymmetric irrep  $(0,0)$  with  $SU(3)$  labels  $(\lambda, \mu)$  such that  $\lambda = 1 - 1 = 0$  is the difference between the number of  $\square$ s in the first and second rows, and  $\mu = 1 - 1 = 0$  is the difference between the number of  $\square$ s in the second and third rows.

Basis states for the irrep  $(\lambda, \mu)$  are denoted  $|(\lambda, \mu) \nu_1 \nu_2 \nu_3; I\rangle$  with  $\nu_i$  the number of photons in port  $i$  and  $\nu_1 + \nu_2 + \nu_3 = \lambda + 2\mu$ . The index  $I$  distinguishes states with the same weight  $(\nu_1 - \nu_2, \nu_2 - \nu_3)$  belonging to different irreps of the  $SU_{23}(2)$  subgroup of  $SU(3)$ . In this notation, the three-photon state decomposes into

$$\begin{aligned} |1(\omega_1)1(\omega_2)1(\omega_3)\rangle &= \frac{1}{\sqrt{6}} |(00)000; 0\rangle + \frac{1}{\sqrt{6}} |(30)111; 1\rangle \\ &+ \frac{1}{2} |(11)111; 0\rangle_1 + \frac{1}{\sqrt{12}} |(11)111; 1\rangle_1 \\ &- \frac{1}{\sqrt{12}} |(11)111; 0\rangle_2 + \frac{1}{2} |(11)111; 1\rangle_2. \end{aligned} \quad (16)$$

The  $SU(3)$  irrep  $(1,1)$  occurs twice in Eq. (15); thus, an additional subscript (1 and 2) is needed to denote basis states that belong to these distinct copies of  $(1,1)$ . This input transforms as  $R(\Omega)|1(\omega_1)1(\omega_2)1(\omega_3)\rangle$  and can be expanded in terms of the appropriate  $SU(3)$   $D$ -functions.

The Young tableaux also label the representations  $\begin{array}{c} \square \square \square \\ \square \square \square \end{array}$ ,  $\begin{array}{c} \square \square \\ \square \square \end{array}$  and  $\begin{array}{c} \square \\ \square \\ \square \end{array}$  of  $S_3$  (the six-element permutation group of three objects). Characters of  $\begin{array}{c} \square \square \square \\ \square \square \square \end{array}$ ,  $\begin{array}{c} \square \square \\ \square \square \end{array}$  and  $\begin{array}{c} \square \\ \square \\ \square \end{array}$  are needed to construct the permanent, immanant and determinant of a  $3 \times 3$  matrix [17], respectively. Whereas the connection between coincidences at the interferometer output, the  $D$ -functions, and the permanents is clear [9, 10, 18], it behooves us to find a relationship between the permanent,

immanant and determinant of  $R(\Omega)$  and the  $D$ -functions of irreps of  $SU(3)$ .

Using Young tableaux to denote the corresponding functions of the matrix  $R(\Omega)$  constructed with frequencies of the output modes fixed with respect to those of the input modes, we observe the following.

**Observations 1.** For any  $R(\Omega) \in SU(3)$

$$Per(R(\Omega)) \equiv \begin{array}{c} \square \square \square \\ \square \square \square \end{array}(\Omega) = D_{(111)1; (111)1}^{(3,0)}(\Omega)$$

$$Imm(R(\Omega)) \equiv \begin{array}{c} \square \square \\ \square \square \end{array}(\Omega) = D_{(111)1; (111)1}^{(1,1)}(\Omega) + D_{(111)0; (111)0}^{(1,1)}(\Omega)$$

$$Det(R(\Omega)) \equiv \begin{array}{c} \square \\ \square \\ \square \end{array}(\Omega) = D_{(000)0; (000)0}^{(0,0)}(\Omega).$$

so the full permanent of the general  $3 \times 3$   $SU(3)$  matrix equals the  $D$ -function for irrep  $(3,0)$  with weight 0 input and output. The immanant of  $R(\Omega)$  is the sum of  $D$ -functions for the irrep  $(1,1)$  with weight 0 input and output, and the determinant of  $R(\Omega)$  is just the  $D$ -function for irrep  $(0,0)$ .

**Observation 2.** For  $R(\Omega)_{kj}$  the  $2 \times 2$  submatrix of  $R(\Omega)$  with the  $k^{th}$  row and  $j^{th}$  column removed,

$$Per(R(\Omega)_{kj}) = \begin{array}{c} \square \square \\ \square \square \end{array}_{kj}(\Omega) = D_{(110_k)I_k; (110_j)I_j}^{(2,0)}(\Omega)$$

for  $D_{(110_k)I_k; (110_j)I_j}^{(2,0)}(\Omega)$  the  $D$  function with 0 in output state  $k$  and 1 otherwise, and 0 in the input state  $j$  and 1 otherwise. For instance

$$Per(R(\Omega)_{13}) = \begin{array}{c} \square \square \\ \square \square \end{array}_{13}(\Omega) = D_{(011)1; (110)_\frac{1}{2}}^{(2,0)}(\Omega). \quad (17)$$

In view of Observations 1, we consider measuring coincidences for the monochromatic (continuous-wave) three-photon input state  $|1(\omega_1)1(\omega_2)1(\omega_3)\rangle^S$ :

$$\begin{aligned} &^S \langle 1(\omega_1)1(\omega_2)1(\omega_3) | R(\Omega) | 1(\omega_1)1(\omega_2)1(\omega_3) \rangle^S \\ &= \frac{1}{6} D_{(111)1; (111)1}^{(3,0)}(\Omega) + \frac{1}{6} D_{(000)0; (000)0}^{(0,0)}(\Omega) \\ &+ \frac{1}{3} (D_{(111)1; (111)1}^{(1,1)}(\Omega) + D_{(111)0; (111)0}^{(1,1)}(\Omega)) \\ &= \frac{1}{6} \begin{array}{c} \square \square \square \\ \square \square \square \end{array}(\Omega) + \frac{1}{3} \begin{array}{c} \square \square \\ \square \square \end{array}(\Omega) + \frac{1}{6} \begin{array}{c} \square \\ \square \\ \square \end{array}(\Omega). \end{aligned} \quad (18)$$

As Eq. (18) is covariant under permutation of the output frequencies, detecting photons of frequencies  $(\omega_i, \omega_j, \omega_k)$  in output ports (1, 2, 3) respectively implies that

$$\begin{aligned} D_{(111)J; (111)I}^{(\lambda, \mu)}(\Omega) &\equiv \langle (\lambda, \mu)(111)J | R(\Omega) | (\lambda, \mu)(111)I \rangle \\ &\mapsto \langle (\lambda, \mu)(111)J | (\wp_{ijk})^{-1} R(\Omega) | (\lambda, \mu)(111)I \rangle \end{aligned} \quad (19)$$

with  $\wp_{ijk}(\omega_1, \omega_2, \omega_3) \mapsto (\omega_i, \omega_j, \omega_k)$  a permutation operator, and the action of  $\wp_{ijk}$  on  $SU(3)$  basis states is known [19].

Permuting output frequencies effects permutations of the rows in the basic  $SU(3)$  matrix. The permanent thus remains unchanged; the determinant picks up a sign for odd permutations; and the immanant transforms in a

more complicated way according to the 2-dimensional irrep of  $S_3$ . Equation (18) remains valid provided the above changes are implemented.

The coincidence rate for output modes (1, 2, 3) is

$$P_{111}(\Omega) = \left| \langle 111 | R^\dagger(\Omega) \Pi_1 \otimes \Pi_1 \otimes \Pi_1 R(\Omega) | 111 \rangle \right|^2,$$

which is a function of the two inter-photon delay times  $\tau_1$  and  $\tau_2$  and plotted in Fig. 1 for various values of  $\Omega$  and choices of the three detector spectral terms  $\omega_i$  and  $\sigma_i$ ,  $i = 1, 2$ , and 3. This rate  $P_{111}(\Omega)$  is a sum of six terms, one for each possible permutation of the three frequencies  $(\omega_i, \omega_j, \omega_k)$  of the photons in output channels (1, 2, 3) respectively. Each term is the product of an  $\Omega$ -dependent interferometer term as in Eq. (18) and a detector spectral term as in Eq. (2).

The permanent is invariant under permutation of output frequencies: the coefficient of  $D^{(3,0)}$  is constant for all output frequencies; upon rearrangement,  $P_{111}(\Omega)$  contains a single  $D^{(3,0)}$  function multiplying the sum of all detector terms. Interferometer settings that make  $D^{(3,0)}$  vanish also make the permanent vanish from the coincidence rate, thereby resulting in a dip with respect to delay parameters  $\tau_1$  and  $\tau_2$  when detector terms are chosen to eliminate, by symmetry, the contributions from the determinant and the immanants.

In Figs. 1(a) and (b), we choose  $\Omega$  such that  $D^{(3,0)} = 0$  and  $D^{(3,0)} = -1/4\sqrt{2}$ , respectively. Detector terms are partially symmetric under exchange  $1 \leftrightarrow 2$ , thus extinguishing contributions from the immanants and determinant. As expected, only Fig. 1(a) has vanishing dip at the origin of the plot corresponding to two zero time delays. We also provide two examples of three-photon coincidence rates to demonstrate the complexity of dips that can arise when imperfect sources and detectors are used. In Figs. 1(c) and (d),  $D^{(3,0)} = 0$ , but detector terms are asymmetric: contributions from the immanants and determinant interfere, and we obtain dips at non-zero time delays. Although here we have focused on the rate of obtaining three-fold coincidences corresponding to detecting one photon at each output port, we can easily calculate other coincidence rates such as measuring  $\nu_1$  photons exiting the first port,  $\nu_2$  from the second, and  $\nu_3$  from the third port simply by replacing  $\Pi_1 \otimes \Pi_1 \otimes \Pi_1$  in the calculation of the rate  $P_{111}(\Omega)$  by  $\Pi_{\nu_1} \otimes \Pi_{\nu_2} \otimes \Pi_{\nu_3}$ .

In summary we have used SU(3) group theory to calculate the photon-coincidence rates at the output of a three-channel interferometer given single photons entering each of the three input ports. We employ Young tableaux to decompose the direct product of irreps corresponding to each input photon into a direct sum of symmetric, antisymmetric, and partially symmetric irreps. Our technique provides a powerful calculational tool for modeling and interpreting output data from realistic experiments that are on the cusp of taking the two-photon two-channel Hong-Ou-Mandel dip to a new and excit-

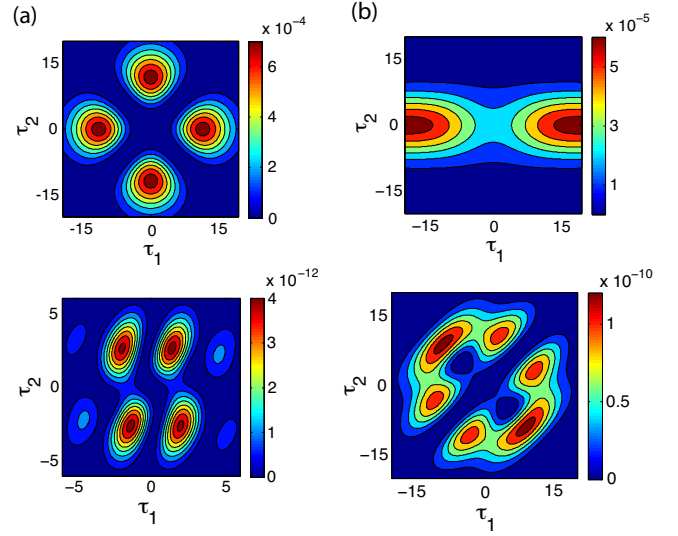


FIG. 1: A plot of the coincidence rate with for three different sets of  $\Omega \equiv (\alpha_1, \beta_1, \alpha_2, \beta_2, \alpha_3, \beta_3, \gamma_1, \gamma_2)$ : (a)  $\Omega = (0, \pi/2, \pi/2, \pi, 0, \pi/2, \pi/2, \pi)$ ,  $\omega_0 = 0$ ,  $\sigma_0 = 0.1$ ,  $\omega_1 = 0$ ,  $\sigma_1 = 0.1$ ,  $\omega_2 = 0$ ,  $\sigma_2 = 0.1$ , and  $\omega_3 = 0$ ,  $\sigma_3 = 1$ , (b)  $\Omega = (0, \pi/2, 0, \pi/2, 0, \pi/2, 0, 0)$ ,  $\omega_0 = 0$ ,  $\sigma_0 = 1$ ,  $\omega_1 = 0$ ,  $\sigma_1 = 0.1$ ,  $\omega_2 = 0$ ,  $\sigma_2 = 0.1$  and  $\omega_3 = 0$ ,  $\sigma_3 = 0.01$ , (c)  $\Omega = (0, \pi/2, \pi/2, 2\cos^{-1}(1/\sqrt{3}), 0, \pi/2, 0, 0)$ ,  $\omega_0 = 0$ ,  $\sigma_0 = 0.5$ ,  $\omega_1 = 3$ ,  $\sigma_1 = 0.2$ ,  $\omega_2 = 2$ ,  $\sigma_2 = 0.2$  and  $\omega_3 = 1$ ,  $\sigma_3 = 0.2$ , and (d) same  $\Omega$  configuration as (a) but with  $\omega_0 = 0.1$ ,  $\sigma_0 = 0.1$ ,  $\omega_1 = 0.95$ ,  $\sigma_1 = 0.11$ ,  $\omega_2 = 0$ ,  $\sigma_2 = 0.1$  and  $\sigma_3 = 0$ ,  $\omega_3 = 0.99$ .

ing regime of single photons entering multi-channel interferometers. Although brute-force calculations can be used to model the outputs from such interferometers, our methods are much more powerful than typical theoretical quantum optics techniques for modeling photonic quantum interferometry, both in terms of making the model tractable and also in making the resultant dips understandable. We have provided a novel and clear connection between the Wigner  $D$  functions for SU(3) and permanents, immanants, and determinants, and this connection is central to understanding the profiles of the photon coincidence dips as depicted in Fig. 1. This connection is especially important in light of the potential application of higher-order photon-coincidence dips to quantum computation such as for the boson sampling problem [10].

We thank D. K. L. Oi, and T. Welshi for helpful discussions. HdG is supported by NSERC and BCS by NSERC, CIFAR and AITF. YYG acknowledges support from an A\*STAR NSS Fellowship.

\* Electronic address: sihui.tan@gmail.com

- [1] C. K. Hong, Z. Y. Ou, and L. Mandel, Phys. Rev. Lett. **59**, 2044 (1987).
- [2] L. Mandel, Rev. Mod. Phys. **71**, S274 (1999), URL

- <http://link.aps.org/doi/10.1103/RevModPhys.71.S274>.
- [3] M. Halder, A. Beveratos, R. T. Thew, C. Jorel, H. Zbinden, and N. Gisin, *New J. Phys.* **10**, 023027 (2008), URL <http://stacks.iop.org/1367-2630/10/i=2/a=023027>.
  - [4] K. N. Cassemiro, K. Laiho, and C. Silberhorn, *New J. Phys.* **12**, 113052 (2010), URL <http://stacks.iop.org/1367-2630/12/i=11/a=113052>.
  - [5] V. Giovannetti, *Laser Physics* **16**, 1406 (2006), ISSN 1054-660X, 10.1134/S1054660X06100033, URL <http://dx.doi.org/10.1134/S1054660X06100033>.
  - [6] K. Mattle, H. Weinfurter, P. G. Kwiat, and A. Zeilinger, *Phys. Rev. Lett.* **76**, 4656 (1996), URL <http://link.aps.org/doi/10.1103/PhysRevLett.76.4656>.
  - [7] R. T. Horn, S. A. Babichev, K.-P. Marzlin, A. I. Lvovsky, and B. C. Sanders, *Phys. Rev. Lett.* **95**, 150502 (2005), URL <http://link.aps.org/doi/10.1103/PhysRevLett.95.150502>.
  - [8] E. Knill, R. Laflamme, and G. J. Milburn, *Nature (Lond.)* **409**, 46 (2001).
  - [9] D. W. Berry, S. Scheel, C. R. Myers, B. C. Sanders, P. L. Knight, and R. Laflamme, *New J Phys* **6**, 93 (2004), URL <http://stacks.iop.org/1367-2630/6/i=1/a=093>.
  - [10] S. Aaronson and A. Arkhipov, in *Proc. of the 43rd annual ACM symposium on Theory of computing* (2011), STOC '11, ISBN 978-1-4503-0691-1, URL <http://doi.acm.org/10.1145/1993636.1993682>.
  - [11] X.-C. Yao, T.-X. Wang, P. Xu, H. Lu, G.-S. Pan, X.-H. Bao, C.-Z. Peng, C.-Y. Lu, Y.-A. Chen, and J.-W. Pan, *Nat Photon* **6**, 225 (2012), URL <http://dx.doi.org/10.1038/nphoton.2011.354>.
  - [12] B. J. Metcalf, N. Thomas-Peter, J. B. Spring, D. Kundys, M. A. Broome, P. Humphreys, X.-M. Jin, M. Barbieri, W. S. Kolthammer, J. C. Gates, et al. (2012), arXiv:1208.4575.
  - [13] R. A. Campos, *Phys. Rev. A* **62**, 013809 (2000), URL <http://link.aps.org/doi/10.1103/PhysRevA.62.013809>.
  - [14] Y. L. Lim and A. Beige, *New J. Phys.* **7**, 155 (2005), URL <http://stacks.iop.org/1367-2630/7/i=1/a=155>.
  - [15] Z. Y. Ou, *Phys. Rev. A* **77**, 043829 (2008), URL <http://link.aps.org/doi/10.1103/PhysRevA.77.043829>.
  - [16] A. B. Klimov and H. de Guise, *Journal of Physics A: Mathematical and Theoretical* **43**, 402001 (2010), URL <http://stacks.iop.org/1751-8121/43/i=40/a=402001>.
  - [17] D. E. Littlewood, *The Theory of Group Characters and Matrix Representations of Groups* (Oxford, Clarendon Press, 1950), 2nd ed.
  - [18] S. Scheel, arXiv:quant-ph/0406127v1 (2004).
  - [19] D. J. Rowe, B. C. Sanders, and H. de Guise, *J. Math. Phys.* **40**, 3604 (1999).